Hindawi Publishing Corporation
Journal of Materials
Volume 2013, Article ID 287853, 8 pages
http://dx.doi.org/10.1155/2013/287853

Research Article

Morphological and Cell Growth Assessment in Near Dense Hydroxyapatite Scaffold

Florencia Edith Wiria,[1] Bee Yen Tay,[1] and Elaheh Ghassemieh[2]

[1] *Singapore Institute of Manufacturing Technology, 71 Nanyang Drive, Singapore 638075*
[2] *Department of Mechanical Engineering, The University of Sheffield, Sir Frederick Mappin Building, Sheffield S1 3JD, UK*

Correspondence should be addressed to Florencia Edith Wiria; florencia@simtech.a-star.edu.sg

Received 27 November 2012; Revised 1 February 2013; Accepted 1 February 2013

Academic Editor: Amit Bandyopadhyay

This paper reports the preliminary results on the morphology of low porosity hydroxyapatite scaffold and its compatibility as a substrate for osteoblast cells. Although having low porosity, the hydroxyapatite scaffold was found to be capable of sustaining cell growth and thus assisting bone ingrowth. Due to the low porosity nature, the scaffold provides higher strength and therefore more suitable for applications with load-bearing requirements such as spinal spacer. The hydroxyapatite scaffolds are prepared via powder processing techniques, using a combination of wet mixing, powder compaction, and sintering processes. The scaffold porosity is estimated via image analysis and micro-CT, which detect porosity level of approximately 16% and pore size of 13 μm. Cell culture investigation demonstrates that the hydroxyapatite substrate is able to provide favourable cell attachment and collagen matrix production, as compared to the commonly used cell culture control substrates. These results indicate that despite the low porosity in the hydroxyapatite scaffolds, they do not hinder being a preferred substrate to provide conducive environment osteoblast cell growth.

1. Introduction

Over the years, many healthcare products related to the improvement of a person's wellbeing as one ages have seen an increase in demand [1]. One of the examples is the use of an artificial implant to replace dysfunctional body parts or to assist the healing process of a diseased body part. Artificial bone implantation has an advantage over the use of autograft (implant sourcing from the same individual) or allograft (implant sourcing from different individual), mainly due to the limited source of bony parts that can be removed and reimplanted. Secondly, autograft and allograft require secondary operations to perform organ removal from the donor site and implantation into the targeted site. Therefore, artificial materials have been researched for bony implant purposes.

In the context of bone-related diseases, hydroxyapatite (HA) has been widely used for bone replacement material due to its similarity in composition with respect to bone. The composition of bone mineral is comparable to sintered HA. The mineral component of bone is a biological apatite, where carbonate substitutes phosphate ions by about 3–5 wt.% [2].

HA has been reported to have bioactivity nature and thus assists integration and interaction of osteoblast with the implants [3]. Apart from its compatibility with osteoblast, HA surface is biocompatible with several other types of cells, such as macrophages, fibroblasts, osteoclasts, and periodontal ligament cells [4]. This makes the potential applications of HA even wider.

There are typically two types of HA being researched, namely, dense and porous HA. Both dense and porous types of HA have been applied in many biomedical applications. Dense HA is usually referred to as HA implants with porosity up to 5% and pore size of approximately 1 μm [4]. It is the most commonly used material in the case of bone substitution for the ear, such as for ossicle (small bone in the middle ear) connection. The advantage of dense HA is its excellent biocompatibility with minimal risk of resorption due to its slow dissolution rate, even among other calcium-phosphate ceramics [5]. Its precipitation rate is also amongst

the slowest [6]. These properties give dense HA an edge over highly porous HA for implant or bone replacement applications that are needed for longer period of time. Dense HA also provides sufficient mechanical strength, as compared to porous HA which is much more susceptible to breaking *in vivo* [7, 8]. Applications of dense HA include a spacer in a disc space, percutaneous access assist devices for continuous ambulatory peritoneal dialysis, and optical examination of internal tissues and maxillofacial reconstruction [4, 9, 10]. However, no osteoconduction occurs in dense HA as the component is lacked in porosity.

The current research focuses on the use of near dense HA structures. By having porosity, however minimal, the HA structures will be able to maintain their advantage of assisting cell ingrowth and osteoconductive properties, but at the same time, the structure is mechanically strong enough to withstand breakage. A dense HA spacer for cervical spine is one of the several applications that would benefit from a near dense HA structures with porosity to a certain degree. A clinical outcome of a dense HA spacer was previously reported as equal to autologous iliac crest interbody fusion and that patients who underwent the HA fusion had less need for secondary operation due to plug slippage [7]. With the introduction of porosity, HA fusion in an implant could be further improved without sacrificing its mechanical strength.

HA scaffold is typically prepared from axial powder compaction of HA powder, followed by binder removal process and further densification of the HA material [4, 11, 12]. To produce straightforward components, axial powder compaction produces little material waste, and production can be carried out at a high rate [13]. Densification processes can be carried out by pressureless sintering, hot isostatic pressing, and microwave sintering [14, 15].

In this research study, low porosity HA scaffolds are prepared via wet powder mixing process, followed by pressureless sintering for the pore former removal. The samples are then characterized and tested for their morphology using microcomputed tomography and image processing. The potential cell growth on the manufactured scaffolds is also tested using MTT assays and collagen staining quantification.

2. Materials and Methodology

Hydroxyapatite (HA) powder was supplied by Himed (powder size distribution of D10 = 95.95 μm, D50 = 145.6 μm, and D90 = 227.6 μm). Corn starch was supplied by Yiak Say Hang Food Industries. The starch particle size was estimated using scanning electron microscope (SEM), and the average particle size was 10 μm.

2.1. Hydroxyapatite Scaffold Fabrication. The scaffold was processed via powder processing route. HA powder was first mixed with corn starch, as a binder-cum-pore forming agent, with the percentage of 80 weight (wt.)% of HA and 20 wt.% of starch. The starch was first dissolved in warm water (70°C) while continuously stirring the solution. The HA powder was added little by little into the dissolved starch solution. Deionized water was added to the solution. The subsequent mixing process was carried out in a jar mill (Gardco 764 AVM) for 3 hours at 120 rpm. Alumina balls were used in the mixing process, with the powder-to-ball mass ratio of 1 : 4.

The HA/starch solution was then air dried for 48 hours and pulverized in room temperature by crushing and grinding the dried HA/starch cake using a mortar and pestle. The HA/starch powder was then compacted with the force of 49.03 kN. The pellets were subsequently subjected to thermal debinding-cum-sintering process (CM Rapid Temp Furnace) in atmospheric environment. The starch was burnt out from the green part during the debinding stage. The debinding process was conducted at holding temperatures of 250°C, 300°C, and 600°C for 1 hour at each holding temperature to ensure complete removal of the binder. The subsequent sintering was performed at 1250°C for 2 hours. The final manufactured scaffolds were 24.4 mm in diameter and 4.8 mm in height.

2.2. Morphological Study

2.2.1. Surface Porosity Evaluation. Surface porosity of the scaffolds was evaluated using SEM (Leica S360) and image analysis (Adobe Photoshop Element v.3). The samples were first gold coated (sputter coated SC7640) prior to SEM inspection using EHT supply of 15 kV. Seven distinct areas ($n = 7$) were taken to obtain porosity using image analysis technique. A grey scale threshold with the limit of 115 was performed, and the resultant image was binarized. The porosity was obtained from the histograms of grey scale. The reported final porosity was obtained by averaging the porosity values of each image analysis.

2.2.2. Internal Morphological Test. Internal morphological test was conducted using microcomputed tomography (micro-CT, SkyScan 1172) scans carried out with sample sized $2 \times 2 \times 2$ mm. The pixel size used was 4.3 μm. Reconstruction of the scan to image was carried out with conversion values from 0 (minimum) to 0.12 (maximum). Analysis was carried out using CTAn software with region of interest volume (ROI) in the form of a circular area of 1 mm diameter with 1 mm thickness. Six ROIs were taken to obtain the porosity measurement ($n = 6$), with histogram greyscale limit set from 75 to 125. These ROIs extend through the data set slice by slice to create 3D volume of interest (VOI), which can then be analysed. The values of interest produced for the processed VOIs are pore size, closed porosity, open porosity, and total porosity.

The porosity of the scaffold was indirectly calculated from the sample's true volume, measured using a pycnometer (Micromeritics, AccuPyc 1330). Ten samples were used for the measurement ($n = 10$).

2.3. Hardness Measurement. Hardness measurement of the HA scaffolds was conducted using a Vickers microhardness measurement tool (MMT-X3, Matsuzawa Co., Ltd.). A diamond indenter with 490.3 N load was used to indent eight

distinctly different locations on the scaffold ($n = 8$). These readings were calculated to obtain the average and standard deviations of the final hardness.

2.4. Cell Culture Experiment. The scaffolds were sterilized using autoclave process. Subsequent to the sterilization, the scaffolds were washed with phosphate buffer saline (PBS) and were conditioned with the cell media (Invitrogen, MEM Alpha Medium, with Ribonucleosides and Deoxyribonucleosides, cat. 22571).

The scaffolds were divided into two groups, each having three scaffolds ($n = 3$). The cells used were MLO-A5 osteoblastic cells, which is a postosteoblast and preosteocytes type of cells. Group 1 was seeded with cell density of 50,000 cells per scaffold. Group 2 was seeded with cell density of 500,000 cells per scaffold. Each scaffold well was given 4 mL of media, sufficient to cover the whole scaffold. Three controls were used for each of the group. Each control well was given 2 mL of media, which was typically sufficient for cells seeded on 6-well culture plates. Media for cells cultured on both scaffolds and control wells were changed every 3 days. The cell-seeded scaffolds and controls were kept in a static incubator for 7 days. Microscope observations were carried out to ensure that there were no contaminations and that the cells were growing well. The examination of the cell culture result was carried out by two methods, namely, MTT assay and collagen staining observations.

MTT ((3-(4,5-dimethylthiazol-2-yl)-2,5-diphenyltetrazolium bromide) concentration of 0.5 mg powder (Sigma) per 1 mL of PBS was used. The culture plates were incubated at 37°C for 1 hr. Subsequently, the MTT solution was removed off the plate. Acidified isopropanol (prepared by mixing 25 μL of concentrated HCl to 20 mL isopropanol) was given to the scaffold to elute the stain and form the purple formazan. Two samples were taken from each of the purple formazan resulting from the scaffolds and control wells. The optical density was then obtained using a spectrophotometer (Bio-Tek ELx800), using 540 nm wavelength.

Collagen stain was prepared by mixing a solution of sirius red (direct red 80, Fluka) 1 mg/mL in saturated picric acid (Fluka). The samples were washed with distilled water prior to addition of the collagen stain. The immersed samples were then shaken at room temperature overnight. Following that, the samples were washed with distilled water until the red coloring stopped eluting. Subsequently, the samples were destained with a mixture of 0.2 M sodium hydroxide (Sigma) and methanol in a ratio of 1 : 1 and were mildly shaken for 15 minutes at room temperature. Two liquid samples were taken from each solution of the scaffolds and control wells, such that the density could be read. The optical density was then measured using a spectrophotometer (Bio-Tek ELx800), using 490 nm wavelength.

3. Observation, Results, and Discussion

This section discusses the observations gained from the surface porosity, micro-CT, and *in vitro* cell culture examinations.

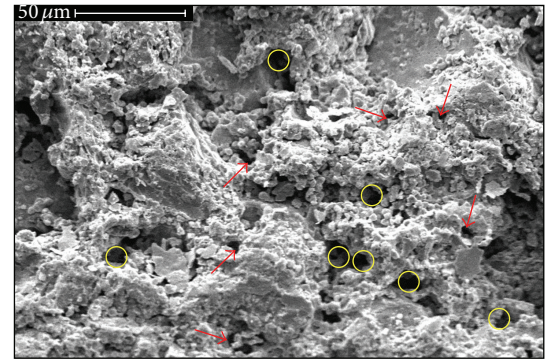

Figure 1: Cross-section image of the HA samples.

Table 1: Micro-CT measurement result.

	Measurement
Pore size	13.21 μm ± 0.35 μm
Closed porosity	8.35% ± 0.78%
Open porosity	8.07% ± 1.24%
Total porosity	15.76% ± 0.53%

3.1. Porosity Analysis. SEM micrographs were used to estimate the surface pore size and porosity level of the scaffold. Figure 1 shows the cross-section area of the sintered HA samples. The image also shows voids that are approximately 10 μm in diameter, as indicated by the circles. These voids are presumably the pores created by the pore forming agents during the debinding process. There are also voids with irregular shape and size smaller than 10 μm, as shown by the arrows. These voids were caused by the sintering and densification process of the HA powder. As the pore-forming agents were burnt, they leave behind empty space. These voids were then taken up by the HA powders that are being sintered, such that connections among the HA particles were formed irregularly. These observations show that the debinding-cum-sintering processes is sufficient to remove the pore-forming agents, as well as to sinter the HA skeleton.

Images of the sample surface were used in the image analysis to estimate the porosity of the scaffolds. Figure 2(a) shows a typical SEM image used of the sample's surface area for surface porosity measurement using image analysis, with the inset showing typical pores found on the scaffold surface. Figure 2(b) shows the analyzed image, with the black contrast colour highlighting pore locations on the scaffold's surface. The image analysis approximated the HA surface scaffold porosity to be 15.08% (±0.90%).

Further analysis with the micro-CT confirms the porosity estimation of the HA scaffold within its volume. Micro-CT estimates the morphological parameters of the scaffolds, such as the porosity and average pore size. The micro-CT measurement result is reported in Table 1, and a section of the HA sample used for the micro-CT porosity analysis is shown in Figure 3.

Micro-CT shows that the total porosity of the sample is 15.8% (±0.5%). This porosity is approximated to be a combination of open porosity and closed porosity. Open porosity

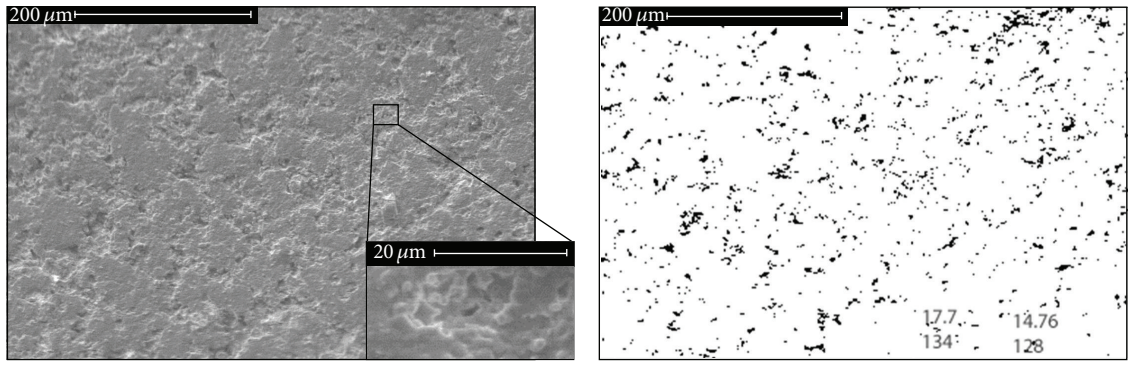

(a) (b)

Figure 2: Typical image analysis of HA scaffold. (a) Micrograph of surface structure (magnified 200 times); inset: typical pores on scaffold surface (magnified 1000 times). (b) Surface porosity of the scaffold, highlighted by the black contrast colour.

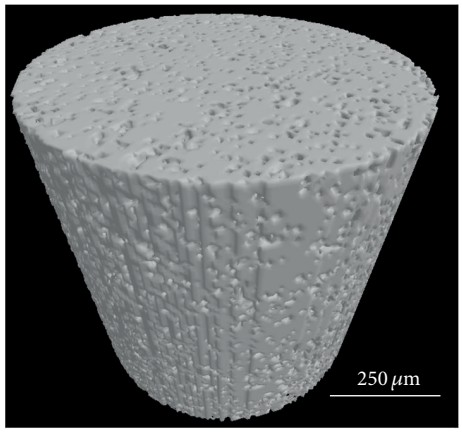

Figure 3: Micro-CT image of the HA sample.

refers to the pores that are interconnected between one another, and closed porosity refers to isolated pores within the scaffold.

The total porosity is shown to be almost evenly divided between the open and closed porosities. It indicates that there are similar amount of both interconnected and isolated pores. Assuming that the pore-forming agents were evenly distributed in the scaffold during the processing, the isolated pores would be predominant in the scaffold. However, the micro-CT finding showed that approximately half of the porosity was open and interconnected pores. There were two reasons of this finding. Firstly, there were pore formers that were not homogenously mixed, presumably during the wet mixing process. Secondly, densification of HA typically starts at temperature range from 700 to 800°C [16]. To ensure complete removal of the pore-forming agents, the debinding process was held at temperature 600°C. Hence, there are voids left by the pore-forming agents, which allow the HA particles to rearrange themselves in temperature range from 600 to 700°C. During the particle rearrangement, there could be movements of the HA particles such that interconnected pores are formed. However, as the range of temperature allowing the particle rearrangement was relatively short, there were limited interconnected pores formed, resulting in the remaining isolated pores.

To further verify the porosity analysis, the porosity of the HA samples ($n = 3$) are calculated indirectly with the help of a pycnometer. The porosity measurement was based on the following formulation:

$$\text{porosity\%} = \left(1 - \frac{\text{true volume}}{\text{bulk volume}}\right) \times 100\%. \quad (1)$$

The pycnometer measures the sample's true volume, whereas the bulk volume is calculated from the measured height and diameter of each sample. The average porosity obtained from the measurement was 22.7% (±2.96%).

It is noted that there is a difference between the porosity calculated using the pycnometer and the porosity estimated by both image analysis and micro-CT. One of the main sources of differences is that there could be due to the loss of data resolution and incorrect identification of the pore edges during the CTAn analysis of the micro-CT volume of interests. Hence, the total pore areas and volume could be underestimated.

From the micro-CT, the average pore size of the HA scaffolds is analyzed to be 13 μm. This pore size estimation is expected as the pore-forming agent used is approximately 10 μm in diameter. Therefore, assuming that the pore-forming agents were removed completely and the HA particle rearrangement during sintering was minimal, the pore formers would leave behind void volumes similar to their original size.

The porosity and pore size obtained from the process are well below the so-called definition of highly porous structures that are commonly reported, with minimum 40% porosity and pore size of 100 μm and above [17–20]. This clearly indicates that the selection of pore formers and ratio between the pore former and main material, as well as sintering process parameter, are able to construct HA samples with lower porosity.

3.2. Hardness of the Scaffolds. The HA samples were found to have microhardness property of 5.28 (±1.08) GPa. This

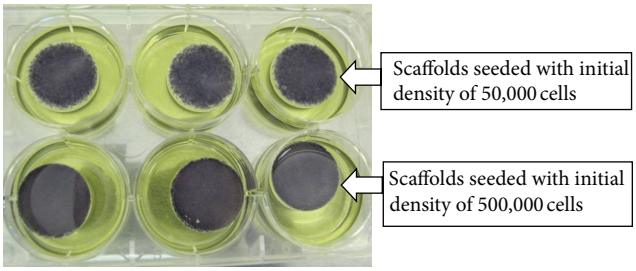

Figure 4: HA scaffolds after MTT staining.

hardness property is distinctively higher compared to similar HA scaffold with porosity of 20%, as reported by Ma et al. [21]. It was noted, however, that Ma et al. applied a different processing technique to prepare the HA scaffold green part. Multiple deposition of HA colloid was carried out using electrophoretic deposition technique in order to obtain bulk HA scaffold. The green part was sintered at 1200°C, which was slightly lower as compared to the sintering temperature used in the current study. However, the sintering duration is the same as the one used in the current study. The electrophoretic disposition technique employed in the previous report could have produced green part with lower strength as compared to the powder-processing techniques utilized to fabricate the HA samples in this paper, as the the deposition was carried out by repeating single deposition several times and as such allowing the possibility of delamination to occur. Microhardness is an indicator of local structural integrity [22] and is related to the yield strength of a material [23]. As such, this suggests that the HA scaffold processed by the powder compaction has more superior structural integrity as compared to HA samples with similar porosity level prepared by other methods. This is attributed to the formation of a dense strong matrix inside the scaffold.

3.3. Cell Culture Experiments. MTT is a colorimetric assay that is used to qualitatively identify the cell locations in a substrate. This assay measures the reduction of yellow MTT solution by mitochondrial succinate dehydrogenase that is found in live cells. The MTT enters the cells and passes into their mitochondria where it is reduced to an insoluble, dark, purple formazan product. The cells are then solubilized with an organic solvent, and the released dark purple formazan reagent is measured spectrophotometrically. Quantitatively, for a 2D substrate, the colour intensity of the purple liquid indicates the relative number of cells that were alive in the substrate.

After the addition of MTT solution, both the HA scaffolds and control plates showed signs of live cells occupying the space. This was indicated by the purple colour that appeared on the scaffolds and the control plates as a reaction between the MTT solution and live cells, as shown in Figure 4.

As the reduction of MTT into dark purple formazan can only occur in metabolically active cells, the appearance of the dark purple colour is a sign of the cell viability in the scaffolds and on the control plates.

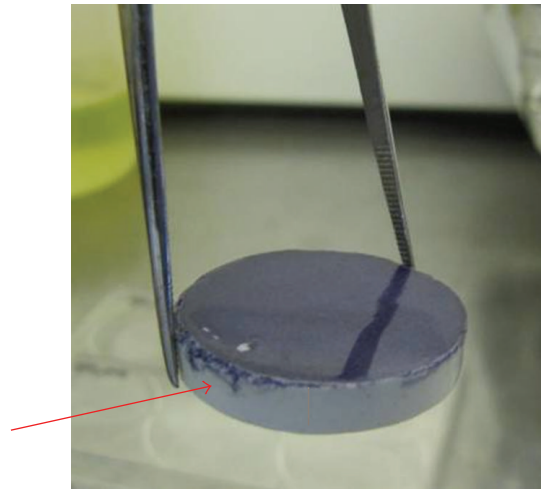

Figure 5: Cells indicated at the scaffold circumference.

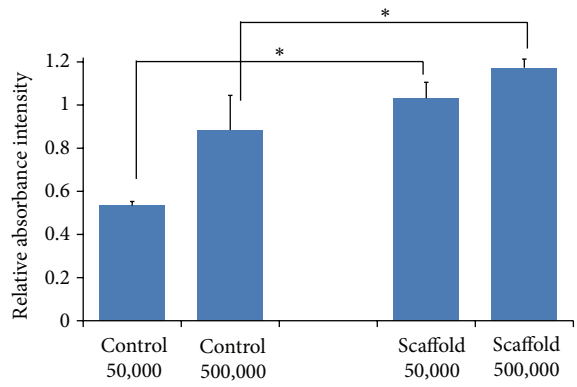

Figure 6: MTT quantification of relative numbers of cells after 7 days of seeding (* indicates significant difference, $P < 0.05$).

It is noted the cells are able to slightly penetrate to the circumference of the scaffolds. It is observed in Figure 5 that the dark purple colour appears at the scaffold's circumference, as pointed by the arrow. This implies that even though the scaffolds has relatively low amount of porosity of 15 to 22%, limited amount of cells could still penetrate into the scaffold's interior. The cellular activity of infiltrating into the scaffold's circumference regardless of the scaffold's low porosity could be due the sintering of the HA that is adopted to produce the samples. Rodrigues et al. reviewed that sintering synthetic HA aids in the proliferation and differentiation of osteogenic cells [24]. In another work, the use of sintered HA suggested that the sintering causes the material's surface to be reactive and hence interact favourably with the seeded osteoblast cells [25]. As such, the sintered HA obtains added chemical attraction to the cellular activity, which attracts cells to infiltrate into the scaffold.

Upon complete elution of the dark purple formazan, the colour intensity from the formazan is read by a spectrophotometer. Figure 6 shows the relative number of cells, quantified by MTT assay, after 7 days of continuous seeding.

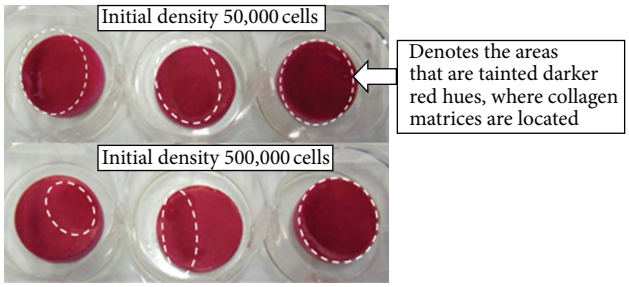

Figure 7: Collagen staining of the HA samples.

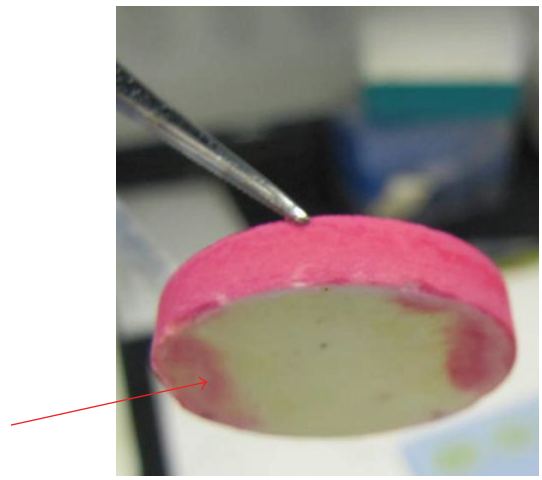

Figure 8: Collagen matrices indicated at the scaffold circumference.

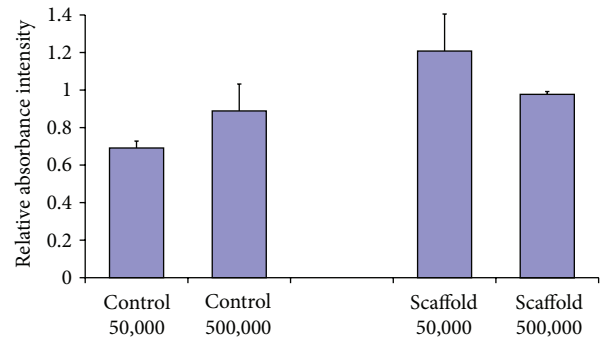

Figure 9: Quantification of collagen matrix production after 7 days of culture.

The numbers 50,000 and 500,000 refer to the initial cell seeding density of 50,000 or 500,000 cells per scaffold or per control plate, respectively.

The MTT reading shows that there is a significant difference between the numbers of cells found on the scaffolds as compared to those found on the control plates. Both readings with 50,000 and 500,000 cell density have $P < 0.05$ confidence level. This result is expected as HA, the scaffold material, is an inorganic mineral with high chemical similarity to that of bone mineral [2, 4]. This result shows that HA is a better substrate to facilitate bone cells growth, as compared to the polymeric control plates, despite of the low porosity of the current HA scaffolds. The HA scaffolds are able to provide more cell growth and proliferation compared to the control plates.

It is noted that the initial amount of cells seeded in the two groups of scaffolds and the controls have a 10-fold difference. However, this is not reflected in the growth and proliferation outcomes after 7 days of culture. This could be explained by the fact that in general cells do not grow in a linear relationship. There are various conditions that affect cell growth. Firstly, overcrowded culture could result in cell death as there is lack of growth space and nutrients from the media. Cells could also fall off the substrate and get washed away in an overcrowded culture. Secondly, there is a limit to the number of cells that a substrate can support for a period of time. Again, this is because the substrate is a static structure which does not have any changes in the dimensions. After a certain period of time, the culture will become overcrowded. Normal cells stop dividing after they reach a certain density. It is understood that after a cell makes contact with other cells on the substrate, specific signal is relayed to inform the cell if all cellular contact points have been satisfied. If all contact points have been satisfied, the genes that signal proliferation are turned off and as such, the proliferation stops [26]. This shows that there is a cell growth saturation point that cannot be surpassed for a specified culture substrate. Therefore, it is not a guarantee that a 10-fold difference in the initial seeding will result in the same fold of cell growth and increase after a certain period of culture time.

As MLO-A5 is an osteoblastic cell type, it would normally secrete collagen when it is proliferating healthily. The collagen staining test is used to measure the amount of collagen matrix formed by the MLO-A5 cells. The collagen staining visual observation is shown in Figure 7. The location where collagen matrices were profoundly found on the scaffold was tainted darker red hues, which is denoted by the dotted lines.

The collagen staining showed that the cells were able to penetrate into the circumference of the scaffolds, as can be seen from Figure 8. However, it was observed that the cell penetration was not in-depth, with mostly limited to the outer circumference of the scaffold. It was seen that the outer circumference of the scaffold was tainted red, and this showed the area that has collagen matrices. However, due to the small pore size and low porosity level possessed by the scaffold, there is a limitation in the spread of collagen matrices into the scaffold. After the baseline reading subtraction, the intensity reading of the collagen matrices amount after 7 days of culture is reported in Figure 9.

In this observation, it is seen that the collagen matrix production in the HA scaffolds was more than that produced on the control substrates. This supports the argument that a 3D HA scaffold, in this case HA scaffold, is a more suitable substrate material, preferred by the bone cells to grow, proliferate, and perform their collagen matrix production function, as compared to the polymeric 2D cell culture plate. This observation was also seen in other work, in which osteocalcin secretion and alkaline phosphatase activity were detected at a significantly higher level on 3D scaffold than

on 2D cell culture plate [27]. This is presumably due to the bioactivity nature of HA, which indicates that the material provides substrates that are capable of attracting cells for bone tissue formation. The bioactive surface is thus capable of significantly facilitating differentiation of osteogenic cells the subsequently and the apposition of tissue matrix *in vitro* [3].

It is also observed that collagen matrices produced by the scaffold with initial seeding density of 500,000 cells were less than that seeded ones with 50,000 cells. This was an interesting finding, as the earlier MTT readings showed that by the end of the 7-day culture, the cells on scaffolds seeded with initial 500,000 cells were able to proliferate more than that of scaffolds seeded with 50,000 cells. Several postulations are given. Firstly, there is a limited area in the scaffold for the osteoblast cells to contain both their proliferation and collagen matrix production activities. When there are too many cells on the substrate, there will not be enough areas for the produced collagen matrices to attach, and the layer of collagen matrices may easily fall off the substrate or get washed away by the PBS. Hence, as the cell quantity in the 50,000-cell scaffolds was less than that of the 500,000-cell scaffold, as was estimated using the MTT test, the cells in the prior scaffolds had more areas to contain the produced collagen matrix. Secondly, when the cells in the 500,000-cell scaffold were occupied in the proliferation activity, it was harder for these cells to work as much to produce the collagen matrices. In the molecular level, there is a certain driving force and energy required for any molecular activities [28]. Therefore, the collagen production could be slowed down if there is less driving energy in the 500,000-cell scaffold due to the continuous proliferation activity.

The cell culture results have confirmed that the HA scaffolds are able to demonstrate its suitability to support anchorage and maintain viability of live cells. Future study would be to continue with the *in vivo* experimental work. It is expected that the low porosity HA will have interactions with its surrounding tissues as normally occurs in implantation of an active bioceramic, as was exhibited elsewhere. A 5-year-HA dental implant retrieved from a human mandible showed a thick bone addition formed on the implant, and chemical bonding existed between the HA implant and the bone [29]. The chemical bonding introduces bioactive fixation between the surface-reactive HA with the bone [30].

4. Conclusions

The current research reported here has shown that low porosity HA scaffold could be well produced using compaction and sintering methods. The microporosity of the HA scaffold has been conducted and has shown that the pore size and porosity level of the scaffold are within the range for a low porosity scaffold. The mechanical hardness strength of the scaffold was also found to be comparable, if not higher than other HA scaffolds with similar porosity value.

The cell culture experiment has shown that HA scaffold is a more preferred substrate material as compared to the polymeric cell culture plate for culturing osteoblast cells. This is despite the standard condition of the cell culture control plates having been treated by vacuum-gas plasma to provide conducive cell attachment environment. The osteoblast cells seeded onto the HA scaffolds are found to yield favourable results in both the numbers of cells and in cellular activity after a certain period of time. This results demonstrate that the HA scaffolds are suitable to support anchorage and maintain viability of live cells. Initial cell seeding of 50,000 MLO-A5 cells is found to be sufficient for culture on the HA scaffolds. This amount of initial cell seeding density is adequate to demonstrate favourable cell growth and proliferation. This initial cell seeding density is also sufficient in order to avoid cell overcrowding for effective collagen matrix production.

It is noted that this scaffold with lower porosity or near dense properties are still capable of providing cell attachment into the pores of the scaffolds, while it simultaneously provides sufficient handling strength to potentially avoid breakage during the implantation. It is hence suggested that this type of HA scaffold could be used as effective bioactive scaffolds for applications that required high strength, such as bone or spinal implant grafts. The future works that could be carried out based on the current study is to evaluate the degradation and resorption mechanisms of the HA scaffold *in vitro*.

Acknowledgments

The authors would like to thank Dr. Gwendolen Reilly and Dr. Anuphan Sittichokechaiwut (Department of Engineering Materials, The Kroto Research Institute, North Campus, University of Sheffield) for the valuable advice and discussion, provision of the osteoblast cells and cell culture consumables, and assistance in the cell culture process. Dr. F. E. Wiria would like to acknowledge the funding from the British Council Researcher Exchange Programme that provides the collaboration opportunity and the use of micro-CT equipment.

References

[1] M. J. Lysaght and A. L. Hazlehurst, "Tissue engineering: the end of the beginning," *Tissue Engineering*, vol. 10, no. 1-2, pp. 309–320, 2004.

[2] D. Tadic and M. Epple, "Mechanically stable implants of synthetic bone mineral by cold isostatic pressing," *Biomaterials*, vol. 24, no. 25, pp. 4565–4571, 2003.

[3] K. Y. Lee, M. Park, H. M. Kim et al., "Ceramic bioactivity: progresses, challenges and perspectives," *Biomedical Materials*, vol. 1, no. 2, pp. R31–R37, 2006.

[4] R. Z. LeGeros and J. P. LeGeros, "Dense hydroxyapatite," in *An Introduction to Bioceramics*, L. L. Hench and J. Wilson, Eds., vol. 1, pp. 139–180, World Scientific, Singapore, 1993.

[5] O. Malard, F. Espitalier, P. Bordure, G. Daculsi, P. Weiss, and P. Corre, "Biomaterials for tissue reconstruction and bone substitution of the ear, nose and throat, face and neck," *Expert Review of Medical Devices*, vol. 4, no. 5, pp. 729–739, 2007.

[6] P. Ducheyne and Q. Qiu, "Bioactive ceramics: the effect of surface reactivity on bone formation and bone cell function," *Biomaterials*, vol. 20, no. 23-24, pp. 2287–2303, 1999.

[7] P. Ylinen, M. Raekallio, R. Taurio et al., "Coralline hydroxyapatite reinforced with polylactide fibres in lumbar interbody implantation," *Journal of Materials Science*, vol. 16, no. 4, pp. 325–331, 2005.

[8] T. Iguchi, A. Kanemura, A. Kurihara et al., "Cervical laminoplasty: evaluation of bone bonding of a high porosity hydroxyapatite spacer," *Journal of Neurosurgery*, vol. 98, no. 2, pp. 137–142, 2003.

[9] S. Barinov and V. Komlev, *Calcium Phosphate Based Bioceramics for Bone Tissue Engineering*, Trans Tech Publications, Enfield, NH, USA, 2008.

[10] L. L. Hench, "Bioceramics: from concept to clinic," *Journal of the American Ceramic Society*, vol. 74, no. 7, pp. 1487–1510, 1991.

[11] G. With, H. J. A. Dijk, N. Hattu, and K. Prijs, "Preparation, microstructure and mechanical properties of dense polycrystalline hydroxy apatite," *Journal of Materials Science*, vol. 16, no. 6, pp. 1592–1598, 1981.

[12] M. H. Nazarpak, M. Solati-Hashjin, and F. Moztarzadeh, "Preparation of hydroxyapatite ceramics for biomedical applications," *Journal of Ceramic Processing Research*, vol. 10, no. 1, pp. 54–57, 2009.

[13] R. H. Todd, D. K. Allen, and L. Alting, *Manufacturing Processes Reference Guide*, Industrial Press, New York, NY, USA, 1st edition, 1994.

[14] D. S. Seo and J. K. Lee, "AFM analysis of anisotropic dissolution in dense hydroxyapatite," *Ultramicroscopy*, vol. 108, no. 10, pp. 1157–1162, 2008.

[15] J. W. Nicholson, *The Chemistry of Medical and Dental Materials*, Royal Society of Chemistry, Cambridge, UK, 2002.

[16] E. Landi, A. Tampieri, G. Celotti, and S. Sprio, "Densification behaviour and mechanisms of synthetic hydroxyapatites," *Journal of the European Ceramic Society*, vol. 20, no. 14-15, pp. 2377–2387, 2000.

[17] E. Chevalier, D. Chulia, C. Pouget, and M. Viana, "Fabrication of porous substrates: a review of processes using pore forming agents in the biomaterial field," *Journal of Pharmaceutical Sciences*, vol. 97, no. 3, pp. 1135–1154, 2008.

[18] K. A. Hing, S. M. Best, K. E. Tanner, W. Bonfield, and P. A. Revell, "Quantification of bone ingrowth within bone-derived porous hydroxyapatite implants of varying density," *Journal of Materials Science*, vol. 10, no. 10-11, pp. 663–670, 1999.

[19] H.-W. Kim, J. C. Knowles, and H.-E. Kim, "Hydroxyapatite/poly(ε-caprolactone) composite coatings on hydroxyapatite porous bone scaffold for drug delivery," *Biomaterials*, vol. 25, no. 7-8, pp. 1279–1287, 2004.

[20] H. Omae, Y. Mochizuki, S. Yokoya, N. Adachi, and M. Ochi, "Effects of interconnecting porous structure of hydroxyapatite ceramics on interface between grafted tendon and ceramics," *Journal of Biomedical Materials Research A*, vol. 79, no. 2, pp. 329–337, 2006.

[21] J. Ma, C. Wang, and K. W. Peng, "Electrophoretic deposition of porous hydroxyapatite scaffold," *Biomaterials*, vol. 24, no. 20, pp. 3505–3510, 2003.

[22] R. A. Ayers, S. J. Simske, C. R. Nunes, and L. M. Wolford, "Long-term bone ingrowth and residual microhardness of porous block hydroxyapatite implants in humans," *Journal of Oral and Maxillofacial Surgery*, vol. 56, no. 11, pp. 1297–1301, 1998.

[23] G. P. Evans, J. C. Behiri, J. D. Currey, and W. Bonfield, "Microhardness and Young's modulus in cortical bone exhibiting a wide range of mineral volume fractions, and in a bone analogue," *Journal of Materials Science*, vol. 1, no. 1, pp. 38–43, 1990.

[24] C. V. M. Rodrigues, P. Serricella, A. B. R. Linhares et al., "Characterization of a bovine collagen-hydroxyapatite composite scaffold for bone tissue engineering," *Biomaterials*, vol. 24, no. 27, pp. 4987–4997, 2003.

[25] F. B. Bagambisa and U. Joos, "Preliminary studies on the phenomenological behaviour of osteoblasts cultured on hydroxyapatite ceramics," *Biomaterials*, vol. 11, no. 1, pp. 50–56, 1990.

[26] G. M. Fuller and D. Shields, *Molecular Basis of Medical Cell Biology*, Prentice Hall, New Jersey, NJ, USA, 1998.

[27] W. Liu, M. K. Bergenstock, W. Lau, W. Sun, and Q. Liu, "Comparison of osteogenic cell differentiation within 2D and 3D culture systems," in *Proceedings of the 2nd World Congress on Tissue Engineering and Regenerative Medicine*, Seoul, Korea, August-September 2009.

[28] H. F. Noller, "The driving force for molecular evolution of translation," *RNA*, vol. 10, no. 12, pp. 1833–1837, 2004.

[29] M. Ogiso, T. Tabata, T. Ichijo, and D. Borgese, "Examination of human bone surrounded by a dense hydroxyapatite dental implant after long-term use," *Journal of Long-Term Effects of Medical Implants*, vol. 2, no. 4, pp. 235–247, 1992.

[30] L. L. Hench, "Bioceramics," *Journal of the American Ceramic Society*, vol. 81, no. 7, pp. 1705–1728, 1998.